Modeling atmospheric stable water isotopes and the potential for constraining cloud processes and stratosphere-troposphere water exchange

Gavin A. Schmidt,[1] Georg Hoffmann,[2] Drew T. Shindell,[1] and Yongyun Hu[3]

Received 21 January 2005; revised 16 May 2005; accepted 14 September 2005; published 12 November 2005.

[1] Stable water isotope tracers (HDO and $H_2^{18}O$) are incorporated into the ModelE version of the Goddard Institute for Space Studies Atmospheric (GISS) General Circulation Model (GCM). Details of the moist convective parameterisation, cloud phase, background ozone, isotope kinetics and vertical resolution are varied and we examine their impacts, particularly in the upper troposphere (UT) and lower stratosphere. We find that isotopes in precipitation, except in Antarctica, are largely unaffected by these changes and thus are not a useful metric for evaluating model skill above the lower troposphere. Simulated isotopic entry values into the stratosphere over all experiments range between −750 and −600‰ for HDO, and −130 to −90‰ for $H_2^{18}O$, demonstrating that the mixing processes simulated by the model can explain a significant part of the observed offset from pure Rayleigh distillation. Isotope fields are shown to be sensitive to the parameterisation of cloud physics and representation of UT processes and therefore may be useful in constraining modeled cloud physics and mechanisms of stratosphere-troposphere water vapour exchange.

Citation: Schmidt, G. A., G. Hoffmann, D. T. Shindell, and Y. Hu (2005), Modeling atmospheric stable water isotopes and the potential for constraining cloud processes and stratosphere-troposphere water exchange, *J. Geophys. Res.*, *110*, D21314, doi:10.1029/2005JD005790.

1. Introduction

[2] The ratio of stable oxygen and hydrogen isotopes in water have long been used as important tracers of the hydrologic cycle. These ratios are primarily affected by the fractionation occurring at changes of phase - principally in the transitions during surface evaporation or in-cloud condensation. This leads to clear patterns in isotopic ratios in precipitation, atmospheric water vapour, rivers, lakes and oceans which are of great use in distinguishing pathways in the hydrologic cycle [*Gat*, 1996]. Isotopic ratios are here given in standard ‰ notation referenced to Vienna Standard Mean Ocean Water (VSMOW).

[3] General circulation models (GCMs) (including older versions of the Goddard Institute for Space Studies (GISS) model) have been used previously to successfully simulate these isotopes [*Joussaume et al.*, 1984; *Jouzel et al.*, 1987; *Hoffmann et al.*, 1998; *Mathieu et al.*, 2002; *Noone and Simmonds*, 2002] particularly in precipitation for which an extensive database of observations is available [*Rozanski et al.*, 1993; *IAEA*, 2001]. Models though, have had problems in simulating Antarctic precipitation values, particularly the deuterium excess (d-excess, defined as $d = \delta D - 8\delta^{18}O$) [*Hoffmann et al.*, 1998; *Werner et al.*, 1998]. Additionally, variations in simulated upper troposphere fields are large (−500‰ to −700‰ for δD), partly due to the fact that observations of upper tropospheric water isotopes have been sparse [*Ehhalt*, 1974; *Rozanski and Sonntag*, 1982; *Smith*, 1992; *Zahn et al.*, 1998] and have not provided a significant constraint on simulations, and partly due to historically poor simulations of the middle atmosphere. Recently more upper tropospheric/lower stratospheric data has become available from both aircraft measurements (i.e., CRYSTAL-FACE [*Webster and Heymsfield*, 2003]), and from remote sensing [*Moyer et al.*, 1996; *Kuang et al.*, 2003]. The remotely sensed data are primarily for mid-to-upper stratospheric water vapour, but they have been used to infer the isotopic ratio of water entering the lower stratosphere [*Johnson et al.*, 2001a; *McCarthy et al.*, 2004].

[4] Model simulations of cloud water processes [*Del Genio et al.*, 1996, 2005], stratosphere-troposphere exchange (STE) [*Rind and Lerner*, 1996] and methane oxidation in the stratosphere [*Fleming et al.*, 1999], have improved significantly over recent years and mean that a fuller range of isotopic physics can now be included in models. Many important processes (such as the amount of downdrafting, entrainment, or a prognostic cloud water budget) that were previously estimated independently of the cloud scheme [*Jouzel et al.*, 1987], are now treated explicitly, albeit in a parameterised fashion. Together with the increase in available data, more useful model-observation compar-

[1]NASA Goddard Institute for Space Studies and Center for Climate Systems Research, Columbia University, New York, New York, USA.
[2]Laboratoire des Sciences, Climat et l'Environnement, Orme des Merisiers, France.
[3]Department of Atmospheric Sciences, Peking University, Beijing, China.

0148-0227/05/2005JD005790$09.00

isons are now possible. Indeed, now that isotope processes are more tightly coupled to the model physics than before, the possibility arises of using isotopes directly to help validate the base model physics.

[5] We focus on three areas that are of general community interest where isotopic simulations may provide some insight: the impact of cloud parameterisations on the upper troposphere water vapour and tracers, the stratosphere-troposphere exchange of water and the problem of correctly simulating Antarctic deuterium excess, which is (maybe surprisingly) coupled to the other issues. The novelty of this study lies in the use of models that include a well-resolved stratosphere, the consistent variations of the model physics that affect both the climatology and the isotopes and the availabilty of new observational datasets to compare against the model. Most previous published studies were restricted to models with poor representations of the stratosphere, and experiments in which only isotopic physics was altered [i.e., *Jouzel et al.*, 1991].

[6] Understanding the isotopic ratio in Antarctic precipitation is important for interpreting past variations in those ratios as measured in ice cores, such as at Vostok [*Petit et al.*, 1999]. Earlier sensitivity studies [*Jouzel et al.*, 1991] noted that Antarctic $\delta^{18}O$ and d-excess were particularly sensitive to changes in moist convection isotope physics and, crucially, the degree of kinetic fractionation due to super-saturation during condensation to ice in clouds. Non-polar continental values were remarkably unaffected by these choices, a result that is mirrored here. Indeed, tuning of this parameterisation has become the de-facto way to produce the observed d-excess values in Antarctica (see below for details). However, simulations for past time periods, particularly for the Last Glacial Maximum (LGM) show conflicting behaviour for Antarctic d-excess compared to ice core measurements [*Joussaume and Jouzel*, 1993; *Jouzel et al.*, 1994; M. Werner, personal communication]. This may indicate that this tuning procedure is compensating for a deficiency in the physics, which may have a different sensitivity to climate change. We will re-examine this issue here by paying close attention to variations in Antarctic values in the experiments considered.

2. GISS ModelE Description

[7] The model used is the GISS ModelE [*Schmidt et al.*, 2005]. The atmospheric component has similar physics to that in the SI2000 version described in *Hansen et al.* [2002], with improvements to the cloud physics, surface boundary layer, and stratospheric circulation. We use two configurations: the standard control configuration (ORIG) with 20 layers in the vertical and a model top at 0.1 mb, and a more complete stratosphere-resolving model (STRAT) with 23 layers, a model top at 0.002 mb (roughly 85 km) and with parameterised gravity wave drag (GWD). The GWD is imposed as a function of various resolved features: mountain topography, convective events, large scale shear and deformation [*Rind et al.*, 1988]. STRAT also has slightly higher resolution within the troposphere. Estimates of STE in the STRAT model have been validated by using SF_6 and bomb-produced ^{14}C tracers which produce reasonable matches to observations. The ORIG simulation (without GWD and model top near the stratopause) generally has a slightly too strong Brewer-Dobson circulation and higher STE. Note however that both versions resolve the stratosphere better than any previously published isotopic GCM. For reference, the model vertical grid box edges for ORIG are at: 984, 964, 934, 884, 810, 710, 550, 390, 285, 210, 150, 110, 80, 55, 35, 20, 10, 3, 1, 0.3 and 0.1 mb and for STRAT: 984, 960, 929, 884, 819, 710, 570, 425, 314, 245, 192, 150, 117, 86.2, 56.2, 31.6, 17.8, 10, 4.63, 1.46, 0.46, 0.14, 0.03 and 0.002 mb.

[8] In the stratosphere, there is a source of water associated with methane oxidation. This is input using monthly-varying latitude-height source functions derived from a 2-D chemical transport model [*Fleming et al.*, 1999]. Since this is a fixed production rate, an incorrect residence time for air parcels in this zone will lead to incorrect water vapour amounts. In future experiments, we will combine these isotope tracers with interactive methane oxidation, conserving $2CH_4 + H_2O + H_2$, and thus avoiding this particular error. The atmospheric model is run at the relatively coarse $4^\circ \times 5^\circ$ resolution, however, a quadratic upstream scheme [*Prather*, 1986] is used to advect tracers (including water vapour) in a positive definite, conserving and highly non-diffusive way.

[9] Isotopes follow all the physics that affect water vapour in the model (evaporation, condensation, advection, diffusion etc.). In particular, they follow each step and phase change intrinsic to the prognostic cloud liquid water and convection schemes [*Del Genio et al.*, 2005, 1996; *Yao and Del Genio*, 1989] used in the GCM. The moist convective parameterisation represents the spectrum of plumes within a grid box with an entraining and a non-entraining plume. For non-entraining plumes, the water vapour isotopic content is governed by pure Rayleigh distillation and is insensitive to vertical resolution. Surface tracer concentrations are estimated using a planetary boundary layer scheme to extrapolate from the free atmospheric tracer concentration. Tracers are also carried by sea ice, within soil layers, in the snow model and by the river routing and lake modules.

[10] Most fractionation at a change of phase occurs at thermal equilibrium except for three particular cases that have been highlighted in previous investigations [*Jouzel*, 1986; *Hoffmann et al.*, 1998]. Firstly, surface evaporation from open water uses a kinetic fractionation factor dependent on wind speed [*Merlivat and Jouzel*, 1979]. Secondly, there is a kinetic effect that depends on the highly local super-saturation conditions when condensing water vapour to ice. This is parameterised using a super-saturation function $S = 1 - 0.003 * T$ (where T is temperature (°C)) which, at best, is only loosely constrained by data [*Jouzel*, 1986]. It has been set in the ORIG simulation as in previous work [*Jouzel et al.*, 1987; *Hoffmann et al.*, 1998; *Mathieu et al.*, 2002; *Noone and Simmonds*, 2002] to improve the simulation of the deuterium excess in Antarctic precipitation, although we return to this point in the discussion. Thirdly, we use a kinetic fractionation factor when evaporating liquid water into undersaturated air. In raindrops, isotopic equilibrium is maintained for large scale liquid precipitation, but is only partially maintained for moist convective precipitation, since droplets there are assumed to be larger and fall faster [*Jouzel*, 1986]. Note that super-cooled cloud liquid water can exist well below freezing (down to −40°C)

Table 1. Model Experiments

Run	Number of Layers	Model Top, mb	Comment
ORIG	20	0.1	Control
ENT10	-	-	10%/km extra plume entrainment
OZONE	-	-	new lower stratospheric O_3
ICE	-	-	All clouds are ice below −10°C
SUPSAT	-	-	Super-saturation factor 0.004
CAPPA	-	-	*Cappa et al.* [2003] diff. coeff.
NEW	-	-	ORIG+OZONE+SUPSAT + adjustment for radiative balance
STRAT	23	0.002	Strat. model (incl. GWD)

and in such cases we allow full equilibration between the vapour and liquid phases.

[11] Compared to previous simulations with earlier GISS models [*Jouzel et al.*, 1991], we have some significant differences. Firstly, advection of water and isotope tracers is performed using the quadratic upstream scheme [*Prather*, 1986], which is extremely non-diffusive, and superior to the linear upstream scheme [*Russell and Lerner*, 1981] used previously. Secondly, fractionation during condensation in a rising plume is performed assuming that condensate is immediately removed from the air mass. This change was made so that the results of the plume transports were insensitive to vertical resolution and that for a non-entraining case, the results at the plume top match theoretical results for a Rayleigh distillation column. This leads to significantly more depleted water vapour in the upper troposphere than if an equilibrium assumption had been made.

[12] The isotopic composition of the methane-derived water in the stratosphere is set to be that of the source gases, i.e., $\delta D = -70‰$ (from CH_4) and $\delta^{18}O = 23‰$ (from O_2). This has a large impact on the upper stratospheric water isotope composition, but no appreciable effect in the troposphere or lowermost stratosphere. Fractionation effects from the source methane and oxygen [*Ridal and Siskind*, 2002; *Johnson et al.*, 2001a, 2001b], are however important for upper stratospheric isotope ratios and will be assessed in future work.

[13] All experiments were run for 6 to 10 years and the last 5-year mean analysed (Table 1). This is sufficient to stabilise lower stratospheric water concentrations, although the tail of the mid-to-upper stratospheric age distribution takes significantly longer to adjust.

3. Sensitivity Experiments

3.1. Cloud Processes

[14] Cloud processes in models are generally separated into two distinct categories, moist convective processes and stratiform clouds [*Del Genio et al.*, 2005, 1996; *Yao and Del Genio*, 1989, and references therein]. While much of the underlying physics is well understood, the parameterisation of crucial aspects of these schemes at the resolution appropriate for a GCM grid box remains problematic. Factors such as the entrainment into convective plumes, the triggering of moist convection, the detrainment of condensate in anvils, the effects of sub-grid scale turbulence on cloud formation etc. are uncertain to a significant degree. Traditionally model cloud schemes are validated using (among other things) the mean state and variability in TOA radiation fluxes, cloud cover, optical thickness and water vapour.

[15] For moist convection, the GISS model represents the spectrum of plumes within a grid box with an entraining and a non-entraining plume. This has been proved capable of reasonably simulating the observed bimodal distribution of convective mass fluxes in regions of strong convection [*Yao and Del Genio*, 1989]. However, for tracers that have strong dependencies on precipitation efficiency and mixing with the environment (which include water isotopes, but also soluble trace gases and aerosols), the net tracer fluxes may well be skewed by such an approach. Since the fractionation of water isotopes is strongly dependent on the rainout from a rising parcel of air, the isotopic depletion seen in plumes varies strongly as a function of entrainment. It is becoming clear from cloud resolving studies that pure undiluted ascent (such as simulated by the non-entraining plume) does not occur in convective clouds (M. Khairoutdinov, personal communication) and thus observations of water isotopes could in theory provide information on the effective entrainment rate. We therefore examine the dependence of the upper tropospheric water vapour on the entrainment rates into the plumes. We compare the control case (ORIG) where there is a completely non-entraining plume (which acts as a pure Rayleigh distillation column) with a case where the 'non-entraining' plume is also allowed to entrain 10% of it's mass per km (ENT10). This change has only a minimal impact on the climate simulation, but a significant effect on the isotopes.

[16] In the parameterisation of stratiform clouds, the phase of the cloud water is important for deciding whether the condensate is in isotopic equilibrium with the surrounding vapour (the diffusion of water isotopes within ice crystals being too small to allow equilibration), and whether the kinetic fractionation effects during condensation to ice are important. During development of this version of the GISS model, significant effects were seen on the climatology and the isotope fields if the ratio of ice to water clouds was significantly altered. Currently, the phase of a new cloud is determined probabilistically based on an observed probability density function which operates between temperatures of −10 (over land) and −4 (over ocean) to −40°C [*Hobbs and Rangno*, 1985]. Phase changes can also occur probabilistically if frozen precipitation falls into a liquid cloud from above. We therefore performed a sensitivity study (ICE) where we assumed that all clouds below −10°C were ice, similar to the schemes used in previous simulations [*Jouzel et al.*, 1987; *Noone and Simmonds*, 2002; *Mathieu et al.*, 2002].

3.2. Lower Stratospheric Water Vapour

[17] Stratospheric water vapour is important to radiative and chemical processes in the climate and understanding its

variability is crucial to assessing the causes of recent climate changes [*Forster and Shine*, 1999; *Shindell*, 2001]. There are two principle sources of stratospheric water: advection from the troposphere and the oxidation of methane. The stratospheric water specific humidity has been increasing since measurements began in the 1950s [*Evans et al.*, 1998; *Rosenlof et al.*, 2001], at least in part due to increasing methane concentrations in the atmosphere. However, the increases are significantly in excess of that provided by enhanced methane oxidation (although they may have slowed in recent years [*Randel et al.*, 2004]). Thus understanding the processes governing the exchange of water, particularly in the tropics is of great current interest. Mechanisms that have been proposed for tropical STE of water include (a) the gradual ascent of water vapor that undergoes freeze-drying at the tropical tropopause, (b) uplift of thin cirrus ice particles and (c) episodic lofting of ice by deep convective overshoot [*Holton et al.*, 1995; *Holton and Gettelman*, 2001; *Sherwood and Dessler*, 2001] (among others). Each of these above-mentioned mechanisms will have a different isotopic signature (in both HDO and $H_2^{18}O$) and so isotopic ratios have been widely proposed as a useful constraint on the relative strength of these mechanisms [*Moyer et al.*, 1996; *Zahn et al.*, 1998; *Dessler*, 1998; *Keith*, 2000; *Johnson et al.*, 2001a; *Kuang et al.*, 2003].

[18] Observations of water isotopes at the tropopause and lower stratosphere indicate that the most depleted values observed are associated with tropical troposphere-stratosphere transport. The mean isotopic signature of the water entering the stratosphere has been estimated to be $-653 \pm 18‰$ [*McCarthy et al.*, 2004] and $-128 \pm 31‰$ for δD and $\delta^{18}O$ respectively [*Johnson et al.*, 2001a] (error bars are one standard deviation). Smaller scale observations have supported deviations as low as $-900‰$ for δD and $-200‰$ for $\delta^{18}O$ [*Webster and Heymsfield*, 2003] (with data corrections after publication). The mean observations are significantly less depleted than what would be observed in a so-called "Rayleigh distillation" process, where a saturated air parcel is lifted from the surface to the tropopause and all resulting condensate is instantly lost as precipitation. Assuming that the gradual ascent of water vapour in the real world acts like a pure Rayleigh distillation process then implies that other processes (such as those mentioned above) must be responsible for the observed ratios. However, any amount of mixing of previously detrained air or ice will produce less depleted vapour than pure Rayleigh distillation. In this version of the GCM, convection never overshoots (i.e., it only reaches the local neutral buoyancy level) and condensate (ice or liquid water) is not advected, either by the moist convective plume or by the large scale advection. Thus, only the mechanisms of gradual ascent or turbulent entrainment into the stratosphere are simulated. The GCM potentially provides an improved base assumption for estimating the potential for ice lofting and convective overshoot to contribute to the stratospheric water. We should add that moist convection in the model occasionally does cross the 380°K isentropic surface, and deposits moisture above 110 mb. Depending on the definition used, this could be considered the stratosphere (but we note that this is always below the WMO tropopause definition) [*Holton et al.*, 1995].

[19] While not directly involved with the hydrological cycle, changes in the the amount of lower stratospheric ozone can significantly affect the tropopause temperature and hence the cold-trap that is one of the determinants of the incoming stratospheric water vapour. A new ozone dataset compiled from all existing sources was developed while this study was underway [*Schmidt et al.*, 2005]. The OZONE experiment is thus the same as ORIG, but uses the new dataset which has slightly less ozone in the lower tropical stratosphere, and thus a slightly cooler tropopause.

3.3. Isotope Parameterisations

[20] To gauge the importance of the base model changes discussed above compared to uncertainties in the isotope physics, we also describe the impact of two changes that only affect the isotopes. In one case, we adjust the super-saturation function used in calculating the kinetic effects when condensing to ice to be $S = 1 - 0.004 * T$ (SUPSAT). As mentioned above, this is a standard 'tuning' parameter for adjusting the deuterium excess in Antarctic precipitation, however we demonstrate that it has implications for upper tropospheric isotopic ratios as well.

[21] In the second case we examine the diffusivities used in estimating kinetic effects for the isotopes (CAPPA). Recently *Cappa et al.* [2003] suggested that the standard values for the kinetic fractionation during evaporation and the diffusion coefficients used in the kinetic fractionation within clouds [*Merlivat and Jouzel*, 1979; *Jouzel*, 1986] may be incorrect due to the neglect of surface cooling effects in the original experiments. Revised values for the diffusion coefficients also appear to be in line with a priori calculations based on kinetic theory. A number of differences arise in the CAPPA simulation: Firstly, in the parameterisation of kinetic effects due to super-saturation and evaporation into dry air, there is a direct dependence on the ratio of diffusivities of the isotopes. At the surface, we change the *Merlivat and Jouzel* [1979] parameterisation of kinetic effects to one calculated using the same formula but with the new diffusivities (C. Cappa, personal communication).

$$1000(1-k) = A, w < 7\mathrm{m/s}$$

$$B + Cw, w > 7\mathrm{m/s}$$

where A, B, C for $\delta^{18}O$ were (6, 0.285, 0.82) originally and (7.05, 0.485, 0.727) with the Cappa diffusivities. For δD the values change from (5.28, 0.2508, 0.7216) to (3.64, 0.188, 0.275). The net effect is to increase kinetic effects for $H_2^{18}O$, and decrease them for HDO, increasing the deuterium excess in the evaporate. For the same humidity and temperature conditions the Cappa formulation produces a deuterium excess ≈3‰ higher.

[22] We also include a parameterisation of surface cooling effects in the temperature at which the evaporation takes place

$$\Delta T = Q_{net} / \left(0.009 u^* c_p \sqrt{(\rho_w \rho_a)}\right)$$

where Q_{net} is the net downward heat flux, u^* is the surface friction velocity, c_p the specific heat of sea water, and ρ_w, ρ_a

the surface sea water density and surface air density respectively. This formulation is based on an assumption that there is a thin boundary layer where the flux of heat at the surface is balanced by a turbulent flux at the base as in *McPhee* [1992] and is similar to those considered in *Wick et al.* [1996]. This formula gives surface cooling effects of up to 0.5°C consistent with observations of skin temperature/bulk temperature differences. Experiments (not shown) with and without the surface cooling effects show no significant differences in the isotopes, with the bulk of the difference between CAPPA and ORIG due to the change in kinetic fractionation for surface evaporation.

3.4. Combination Experiment

[23] The improvements seen (described below) in the simulation with the new ozone fields and with the change to the super-saturation parameter lead us to perform an additional experiment (NEW = ORIG + OZONE + SUPSAT) that encompasses both changes. This experiment also includes a minor adjustment to the critical relative humidity in the clouds to ensure radiative balance, and so is not as clean an experiment as the other sensitivity tests. However, this configuration is exactly the same as the M20 model described in the ModelE validation paper [*Schmidt et al.*, 2005]. We also ran this model version for a longer time period (20 years) in order to better assess the steady state simulation of mid-to-upper stratospheric water vapour.

4. Observations

[24] We summarise here the sets of atmospheric observations that we use to validate the isotopic simulation. We concentrate particularly on those that may be of use in constraining upper tropospheric values.

4.1. IAEA GNIP Network

[25] Since 1961 the International Atomic Energy Agency (IAEA) has maintained an evolving Global Network of Isotopes in Precipitation (GNIP) stations where water isotopes have been regularly measured. This network has proved invaluable for isotopic model validation. All stations where enough data have been collected to define a reasonable annual weighted mean and seasonal cycle have recently been amalgamated in the ISOHIS database [*IAEA*, 2001]. We have performed our own interpolation of the data onto the GCM grid for easier comparison with model output. Due to the sparsity of the data, zonal or global means are not particularly reliable and so all comparisons are done as means over the grid boxes with data. Individual grid box comparisons are affected by offsets in the topography, land mask and lack of sub-grid scale variations in the model, but the data are enough to give a good sampling of the model behaviour.

4.2. Antarctic Snow Data

[26] Over Antarctica, precipitation measurements are rare. However, recent snow samples are relatively plentiful. These give more useful mean data than episodic precipitation events because of smoothing over individual events due to snow blowing and compaction. The relationship between deuterium and deuterium excess is particularly instructive [*Petit et al.*, 1991; *Hoffmann et al.*, 1998]. Previous work has shown that the relationship seen in the snow samples is particularly sensitive to the super-saturation function and, though to a lesser extent, the vapour trajectory and mixing along it.

4.3. Midlatitude Tropospheric Data

[27] At a few sites in the northern midlatitudes, vertical profiles of isotopes in water vapour have been made [*Ehhalt*, 1974; *Rozanski and Sonntag*, 1982]. While it is unclear how representative they are of mean conditions, enough data came from the tropopause and below to provide some indication of upper tropospheric values. Minima just below the tropopause are around -500 ± 50‰ for δD and values start to increase again above. This had been related to effects of methane oxidation in the stratosphere - a process that is now included in the model (but see the discussion below). A recent correction of these data for wall water effects and sensible relative humidities has been made (see *Ehhalt* [1974] reference for details) and we compare our data against these new profiles.

[28] Scattered in-situ data [*Zahn et al.*, 1998; *Zahn*, 2001] have also been published, which give a small sampling of water vapour isotope ratios near 400 mb over Northern Europe. Minimum values in the troposphere are around -550‰ for δD and -75‰ for δ^{18}O. Stratospheric values (mostly measured in tropopause folds) were significantly less depleted (-280 to -500‰).

4.4. Stratospheric Water Vapour

[29] Apart from a single reliably measured stratospheric profile of water vapour δD [*Pollack et al.*, 1980], most of the information regarding stratospheric water vapour comes from remote sensing. The data do not have sufficient precision to be useful in a direct comparison, but estimates of the mean water vapour isotope ratios coming into the stratosphere at the tropopause (based on tracer-tracer correlations) have been relatively well constrained [*Moyer et al.*, 1996; *Johnson et al.*, 2001a; *McCarthy et al.*, 2004]. We therefore focus on matching these end-members -653 ± 18‰ [*McCarthy et al.*, 2004] and -128 ± 31‰ for δD and δ^{18}O respectively [*Johnson et al.*, 2001a] (error bars are one standard deviation).

[30] When comparing these values to the model it is tempting to simply note the minimum isotope ratio near the tropical tropopause and associate this with the entry value into the stratosphere. Unfortunately, in these simulations at least, this is not the most appropriate value. In all the cases looked at here, the minimum isotope value is not co-located with the minimum water vapour amount (which is generally at higher altitude). We note this is also observed in the CRYSTAL-FACE data [*Gettelman and Webster*, 2005]. Another measure might be the ratio in the flux that enters through the tropical tropopause. However this level is not necessarily easily defined and is variable in time and space. There is also an overlap in the model between the maximum level to which moist convection goes, and the lowest level at which methane oxidation starts (between 110 mb and 80 mb).

[31] The calculation of *McCarthy et al.* [2004] relied on a conserved tracer (in their case total H_2) to extrapolate to the upper troposphere. We therefore use an analagous methodology that uses a conserved quantity relevant to

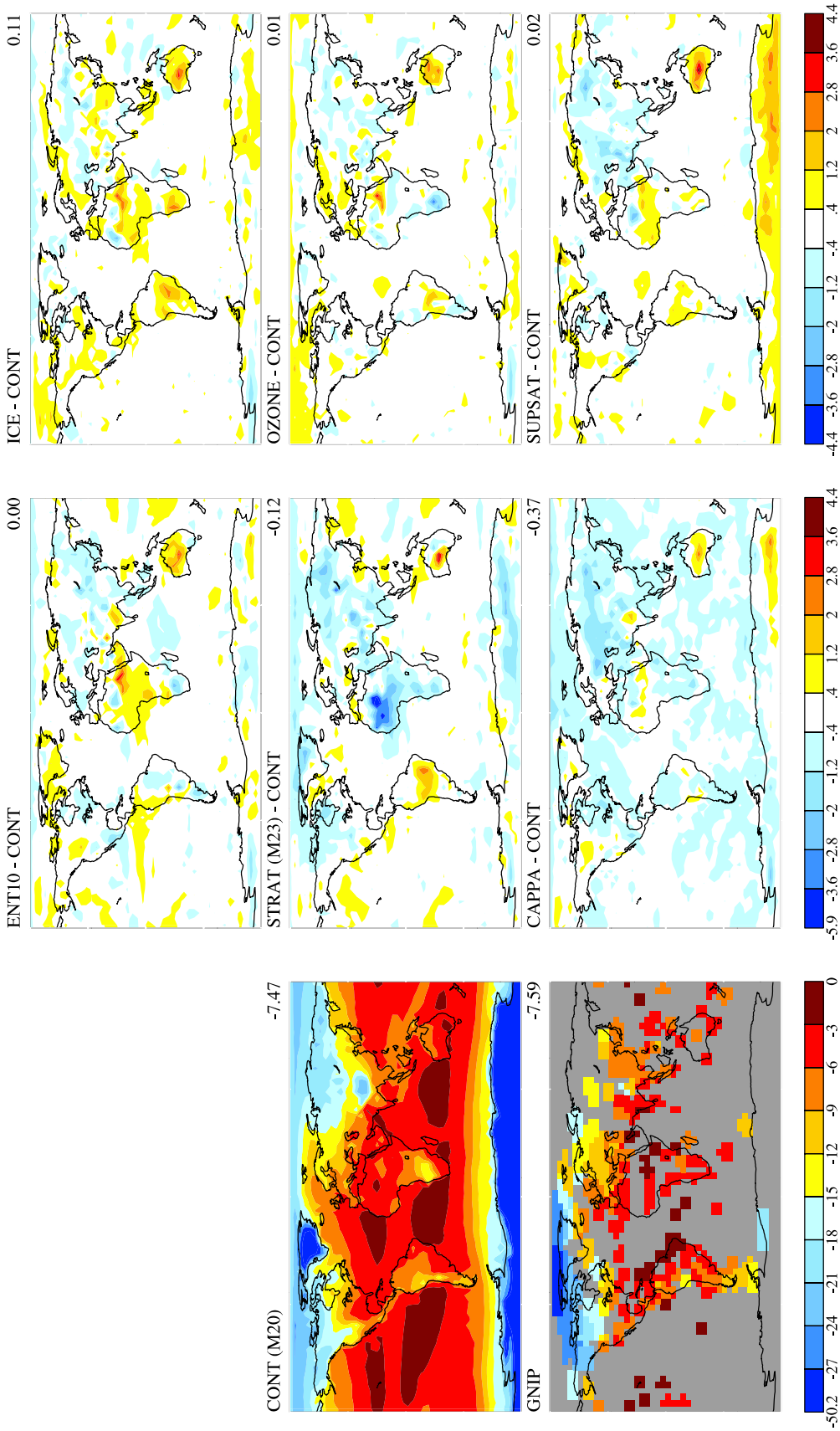

Figure 1. Annual mean $\delta^{18}O_p$ in the control, sensitivity studies and in the GNIP database [*IAEA*, 2001]. The HDO results look very similar to those for $H_2{}^{18}O$ (except for a scaling) and are not shown.

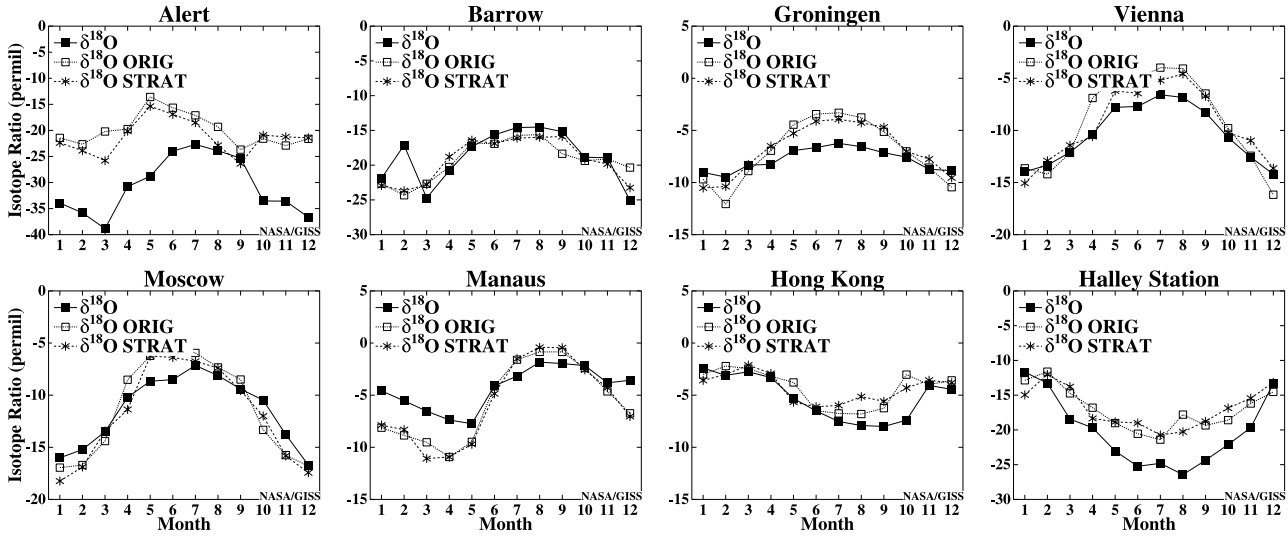

Figure 2. Seasonal cycles of $\delta^{18}O_p$ at selected stations in the ORIG and STRAT models compared to the GNIP database [*IAEA*, 2001]. The HDO results look very similar to those for $H_2{}^{18}O$ (except for a scaling) and are not shown.

these simulations. There are only two sources of water to the stratosphere, and by examining the mass balance for normal water and the isotopes, the isotopic ratio in the stratosphere δ is shown to be linearly related to the inverse of the water vapour mixing ratio Q, i.e.,

$$\delta = \delta_M + Q_{trop}(\delta_{trop} - \delta_M)\frac{1}{Q}$$

where δ_M denotes the isotope ratio of the methane-derived water (fixed in these runs), and Q_{trop} and δ_{trop} are the water vapour mixing and isotopic ratios in the tropospheric source water. Thus air parcels in the stratosphere must lie on this set of straight lines that will depend on the initial δ_{trop} and Q_{trop}. Rewriting the above equation, it is clear that the quantity $\Omega = Q(\delta - \delta_M)$ is conserved. This is to some extent an artifact of these model simulations, nonetheless, this conserved quantity can be used in an analogous way to total H_2 in the real world. If there are different sources (as a function of seasons or location) there will be mixing of these parcels and a homogenization of Ω going up through the stratosphere. Knowledge of the mean upper stratospheric Ω can then be used to extrapolate back to the troposphere.

4.5. CRYSTAL-FACE Measurements

[32] New instrumentation flown for the first time in the CRYSTAL-FACE campaign give the first large scale in-situ measurements of upper tropospheric water vapour and thus are a key new data set for model validation [*Webster and Heymsfield*, 2003]. The instrument used gives the isotopic content of total water (including cloud water or ice) and in the handful of days that the instrument was flown produced some very scattered data. While there are some differences in the water measurements on different instruments, this scatter probably does reflect true small-scale heterogeneity. We note in passing that the extreme depletions (down to −290‰) in the $\delta^{18}O$ reported in *Webster and Heymsfield* [2003] have subsequently been corrected and now show maximum depletions of around −200‰.

[33] For our purposes, we screened the data to look for cases where the relative humidity (with respect to ice) was low (<15%), and where no ice was actually reported. This

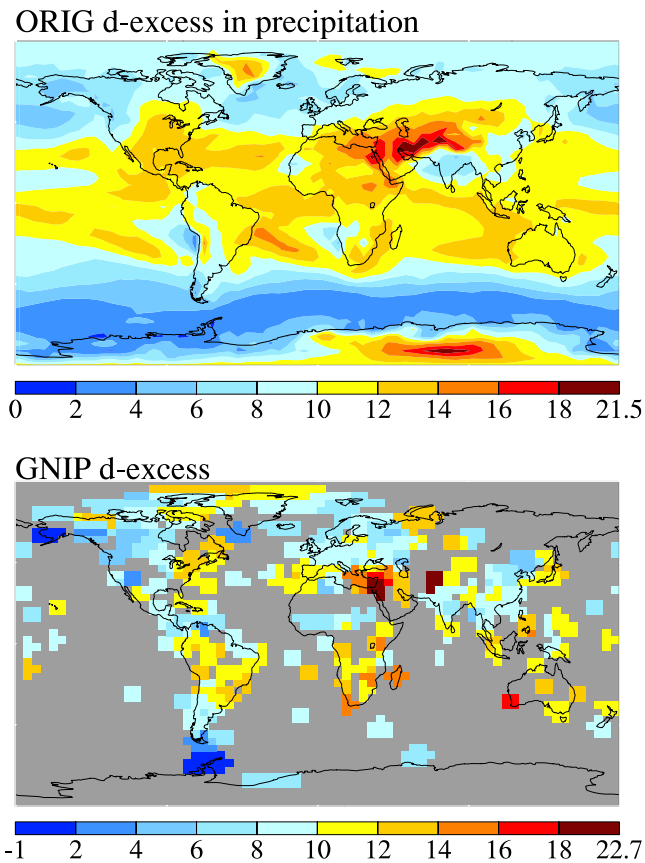

Figure 3. Modeled and observed annual mean d-excess in precipitation.

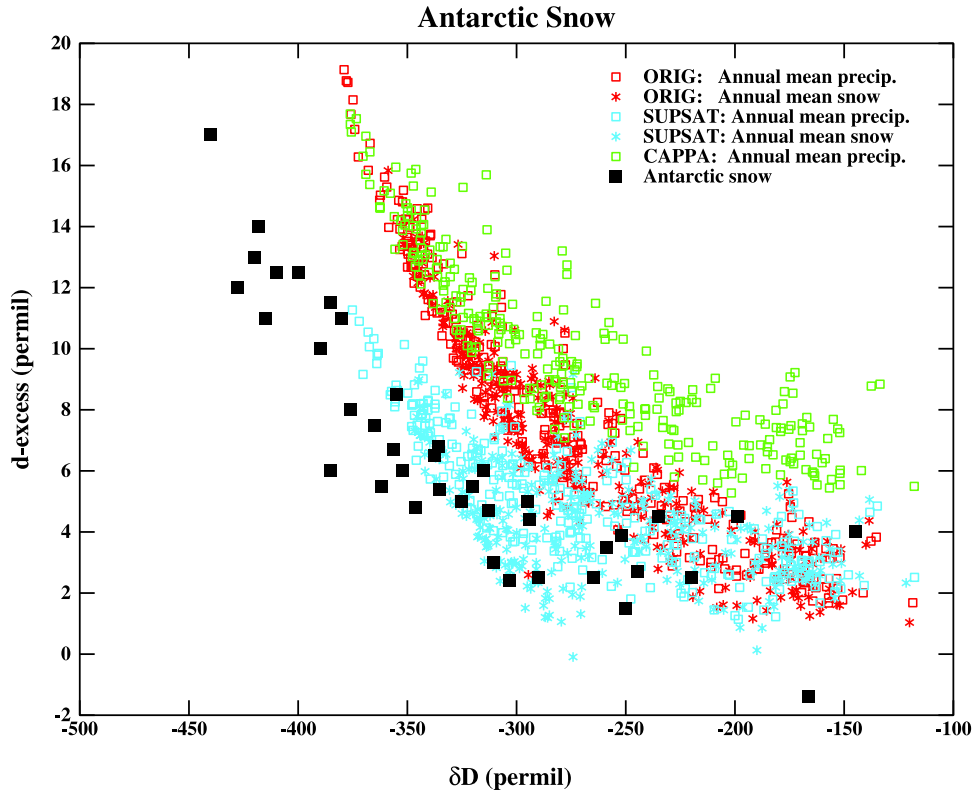

Figure 4. Relationship of δD and d-excess in Antarctic snow and in selected simulations. Observations are from *Petit et al.* [1991] and are nominally multi-annual means.

subset of the data can probably be considered to be pure vapour, but are still widely scattered. In order to make the most suitable comparison, we use instantaneous as well as mean model output and consider the whole tropical tropopause region (not just the few grid boxes around the CRYSTAL-FACE flight path) 28°S–28°N, 285 to 55 mb. This substitutes the model's spatial variability in the tropics for the temporal and sub-grid scale variability in the observations. While not ideal, it does provide a useful comparison.

5. Results

[34] Figure 1 shows the annual mean isotopic content of precipitation $\delta^{18}O_p$ in the ORIG run, the GNIP database and the differences seen in the sensitivity tests. Some of the biases seen are related to biases in the model precipitation fields, but overall the match is extremely good. There are some particular areas of concern in the tropics though. Firstly, the continental values we model in S. America and Africa appear a few permil too depleted, possibly indicative of insufficent onshore advection, and in the case of Amazonia, insufficent mositure convergence over the whole region. An important point to note is that the differences seen in the sensitivity tests are not particularly evident in these precipitation fields.

[35] The selected seasonal cycles shown from ORIG and STRAT (Figure 2) are representative of a number of climate regimes going from the tropical (Manaus 3°S 60°W, Hong Kong 22°N 114°E) to the midlatitude continental (Groningen 53°N 7°W, Vienna 48°N 16°E, Moscow 56°N 38°E) to the high latitude and polar (Alert 82°N 62°W, Barrow 71°N 157°W, Halley Station 76°S 27°W). All show a reasonable seasonality, although offsets in amplitude occur in boxes such as Groningen and Alert where the model representation of the topography and land-ocean mask may be particularly important. In the Manaus dry season, the model under-predicts rainfall consistent with the too-depleted isotope ratios.

[36] In Figure 3 we compare the annual mean d-excess in the control simulation to the values estimated from the GNIP database. Since this is a second-order parameter, there is more noise in the observations, but the overall match is good. The global means are very close, and key patterns, such as the strong north-south gradients in the SH, or the east-west gradient across North America are well captured. The peak d-excess values over the Middle East (due to the importance of kinetic effects when evaporating precipitation into very dry air) are seen in the model as well, although the amplitudes do not match as well, probably due to the lack of d-excess spatial variability in the oceanic source water. The other model simulations (with the exception of CAPPA) show a very similar pattern and are therefore not shown. The CAPPA d-excess is uniformly 3 per mil higher than that shown in the figure and gives a significantly worse match to the observations.

[37] Focusing more on the Antarctic, we compare the model to the observed Antarctic d-excess/deuterium snow measurements (Figure 4) where there are some clear differences in the simulations. We show both the annual weighted mean precipitation values and mean values in the snow itself. Although there is no fractionation assumed during

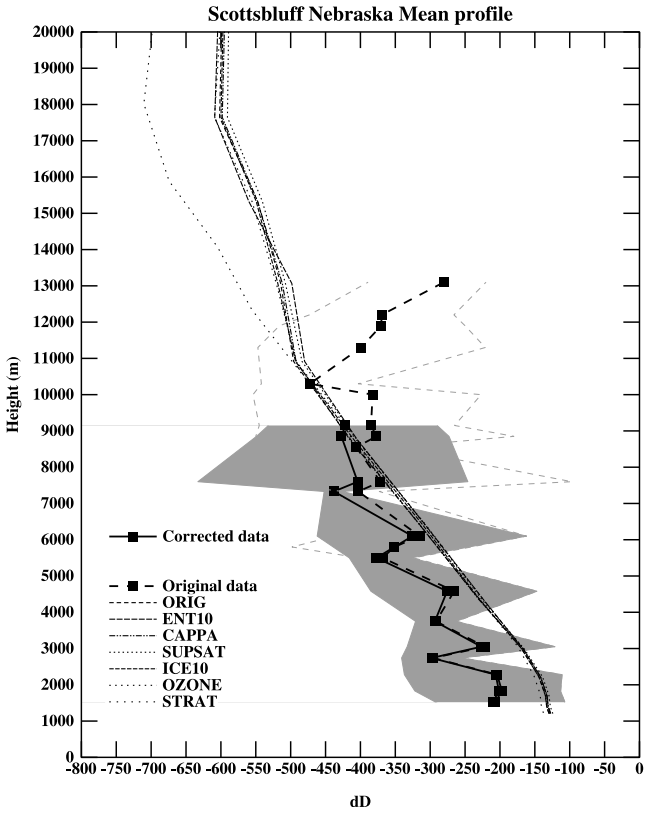

Figure 5. Annual weighted mean δD profiles for each model simulation for Scottsbluff (Nebraska) as a function of height. The mean of the original and corrected data of *Ehhalt* [1974] are shown along with the envelope of the observed values.

sublimation of snow and ice, the snow values are modified from the precipitation by the addition of frost (i.e., direct vapour deposition) and the temporal variability of sublimation which may weight the snow values slightly differently. This leads to snow values with slightly lower d-excess, and higher δD values than for the precipitation, but they not different enough to affect any conclusions drawn from looking solely at the precipitation.

[38] For clarity, only the results from ORIG, SUPSAT and CAPPA are shown in Figure 4, since the other runs are very close (within ±2‰ in d-excess, ±20‰ in δD) to ORIG. If monthly results are looked at, there are more depleted values with a higher d-excess in all cases, but that would not be the appropriate comparison to the observations. Note that the change in SUPSAT only appears to make a difference below −200‰, while the CAPPA results are similar to ORIG in that range, but significantly higher in d-excess in the warmer, less depleted precipitation. Clearly the best match to the data is given by the SUPSAT experiment.

[39] Moving up through the atmosphere, Figure 5 shows clearly that the tropospheric midlatitude profiles are not much different in each simulation. Only STRAT stands out, and then only above 11 km. In the lower troposphere there is some indication that the model values are not sufficiently depleted. Interestingly, the original data published by *Ehhalt* [1974] showed a relatively large increase in δD above the tropopause that had been associated with the importance of methane oxidation in the stratosphere [*Rozanski and Sonntag*, 1982]. Subsequent quality control on the data has led to the higher level values to be rejected. Our simulations include a water source related to methane oxidation, but the impacts are not seen much below 20 km, making it unlikely that the original interpretation could have been correct (had the original data proved valid). This is also consistent with the small differences seen in methane concentrations at that height relative to tropospheric values seen in midlatitude profiles [*Ehhalt and Heidt*, 1973]. The mean tropopause level at this grid point in the simulations is around 15 km (compared to 13 km in the observations) but this alone would not account for the difference.

[40] For the tropical near-tropopause, the comparison of ORIG with the CRYSTAL-FACE data is shown in Figure 6. Qualitatively, the spread in the data and instantaneous model output is comparable, but larger than one might have naively expected (however it is similar to that seen in trajectory modeling [*Gettelman and Webster*, 2005]). There are significantly more outliers in the data, but this might a function of the small spatial scales being sampled. This underlines the significant inhomogeneity of water vapour pathways in the real atmosphere and in the model. Additionally, there are scattered points in both the data and the model that are 'super'-depleted (i.e., isotope values more depleted than pure Rayleigh distillation from the surface). This is possibly due to repeated convective events.

[41] The mean July values are significantly less scattered and shifted toward less depleted values. Note that the maximum depletion (−700‰, at around 12 ppmv) does not coincide with the driest air (near 3 ppmv). Below 7.5 ppmv, in the tropical tropopause layer (TTL) [*Sherwood and Dessler*, 2001], there is evidence of the gradual ascent of the incoming stratospheric air, but it is clear that the starting point for this air is not on the trajectory of undiluted convective plumes rising from the surface. The granularity seen in the zonal means is partly due to the relatively coarse resolution with the three groups of data points corresponding to three different layers in the model, suggesting that the vertical resolution in this region may not be sufficient (this is further discussed below).

[42] Figure 7 shows the annual zonal mean values for the deuterium (HDO) concentrations ($H_2^{18}O$ is similar) for each experiment with a different climate. Both ORIG and STRAT show minima in the upper troposphere (−678 and −743‰ respectively) and a stratospheric tropical pipe (which is slightly leakier in the STRAT case). The OZONE and ENT10 experiments have more depleted lower stratospheres due to a reduction in upper tropospheric water vapour (caused by colder tropopause conditions in OZONE and a downward shift in upper tropospheric moistening by convection in ENT10). The ICE run leads to slight enrichment in the upper troposphere and lower stratosphere. The two experiments with changes purely to the isotope physics (SUPSAT and CAPPA (not shown)) demonstrate that super-saturation parameter has a significant impact in the upper troposphere and above, while the diffusion parameters appear to have very little upper atmosphere impact.

[43] The maxima around 60° in δD between 200 and 300 mb (Figure 7) is a signature of midlatitude isentropic

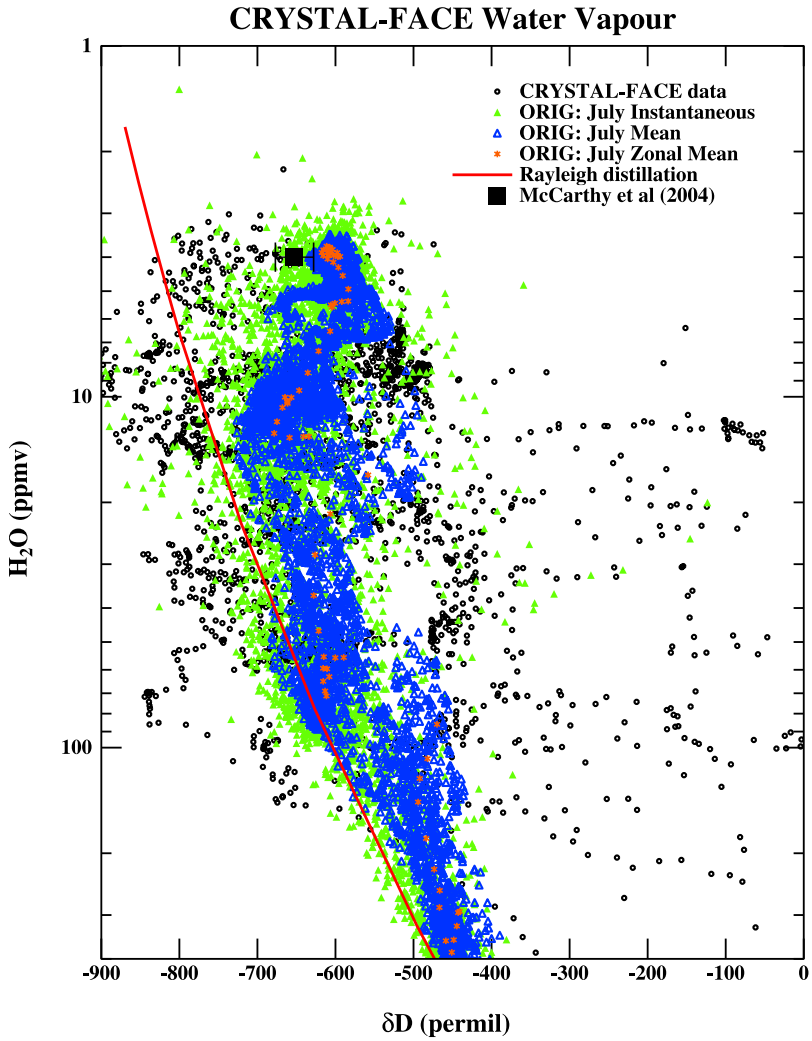

Figure 6. July tropical near-tropopause water vapour. The CRYSTAL-FACE data (July 16–29, 2002, black dots) were screened for low relative humidities and no ice content to ensure a clear water vapour signal [*Webster and Heymsfield*, 2003]. Model output from the ORIG simulation comes from all grid points between 28°S–28°N and 285 to 55 mb. The instantaneous values (green triangles) come from July 1, the weighted mean values (blue triangles) are a 5 July monthly average, and the orange stars are the July zonal means. The Rayleigh distillation curve (red) is calculated using the same kinetic fractionation physics as the ORIG simulation. The inferred entry value for stratospheric water from *McCarthy et al.* [2004] is set at (4.0 ppmv, −653‰).

mixing of tropospheric air occurring in storm systems and tropopause-folding events. The modeled values for this maxima (δD = −385 – −406‰, $\delta^{18}O$ = −54 – −57‰) are close to those observed (δD = −375 ± 75, $\delta^{18}O$ = −50 ± 15‰) [*Zahn*, 2001; *Zahn et al.*, 1998]. Also, the upper stratospheric values around 70 km (0.05 mb) in the STRAT run (δD = −326‰) where the water vapour concentrations are the closest to the HALOE results [*Schmidt et al.*, 2005] are in reasonable accord with results from an interactive chemical 2D model δD = −350 – −330‰ [*Ridal and Siskind*, 2002].

[44] Above, we noted that the isotopic minima seen in the zonal means are not coincident with the minima in water vapour and do not characterise the entry values into the stratosphere (Table 2). To illustrate this further, Figure 8 shows the isotopic ratios plotted against the inverse of the water vapour mixing ratio for tropical boxes above 110 mb (117 mb in the STRAT case). As explained above, in such coordinates the mixing line of stratospheric water with methane-derived input will be a straight line. The intersection of these lines with the upper-troposphere values indicate the range of input values of water vapour and isotopic ratio. In each of the experiments highlighted in the figure, there are a variety of lines, that denote the different seasonal and hemispheric sources of water. The OZONE simulation has a significantly wider spread of entry values than the STRAT simulation for instance. Generally speaking the slightly 'wetter' lines (more to the left) are indicative of southern hemisphere (SH) values, and the dryer lines indicative of the northern hemisphere (NH).

[45] To clarify the processes involved, we show a time-height plot for the mean tropical water over 3 years in the

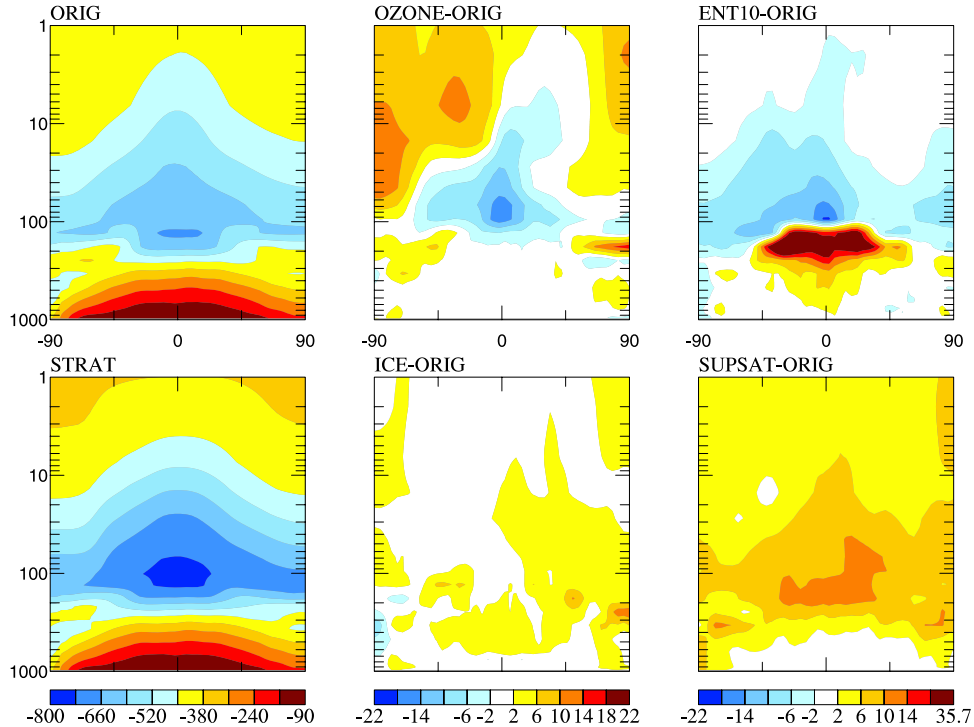

Figure 7. Annual zonal mean concentrations of deuterium (HDO) (‰) as a function of pressure and latitude. The $H_2{}^{18}O$ results look very similar to those for HDO (except for a scaling) and are not shown. The difference in the CAPPA case from the ORIG run is too small to see on these scales.

NEW simulation (Figure 9). These figures show the value of $\Omega - \Omega_0$ at each level, (where Ω_0 is the value for mean tropical upper stratospheric water). The zonal mean tropopause (WMO definition) in these simulations is between 70 and 80 mb in the tropics, and anything below that in these figures can be considered to be part of the TTL. It is clear that in the lowermost stratospheric layer there are no significant sources of water that have the same characteristics as the mean water further up. Instead, there is a range of sources that mix over the lower stratosphere to produce the effective mean values seen. This demonstrates the existence in the model of a 'stratospheric tape-recorder effect' [*Mote et al.*, 1996] in Ω (which is also seen in water vapour [*Schmidt et al.*, 2005]). The blue source (indicating wetter conditions) appears to arise in August though October, and is accompanied by slightly elevated isotope ratios. Curiously, the 'dryer' source (yellow/orange) has two slightly different isotope ratios in the January to March and April to July periods. The fact that the 'wet' excursions in Ω seem larger, is indicative that the 'dry' source dominates (since the weighted mean must be zero by construction). Despite the apparent asymmetry in the timing, the two sources are mainly associated with peak January and July conditions. In January, the outflow from the top of convective atctivity in the SH upper troposphere is efficiently moved up and northward by the upper branch of the Hadley circulation (Figure 10). In July, the convection is not as deep, and the circulation is weaker, leaving the July NH source at a lower level than the January source. It then takes a month or so longer to ascend through the TTL, giving the impression that the 'wet' source was mainly generated in September.

[46] Horizontal slices through the stratosphere (not shown) at all levels indicate that the 'wet' sourced water is found mainly in the SH, while the 'dry' sourced water is predominantly in the north. This is due to the strong cross-equatorial meridional advection in the upper branch of the Hadley circulation.

[47] We quantify the mixing lines by looking at the variations in the tropical mean Ω over an annual cycle for each simulation (Table 3). This slightly damps the extremes seen in the monthly zonal mean values (Figure 10), but is still a good estimate. We take the range of values at 95 mb as representative of the variations of sources in the TTL, and the values at 15 mb as representative of the weighted mean stratospheric values. Given the isotopic ratio of the methane-derived water assumed here (−70‰, and 23‰ for the HDO and $H_2{}^{18}O$ respectively), we can then estimate the approximate water and isotope values at the intersection of these lines (i.e., the dark blue line in Figure 8). This intersection does not define the actual entry values, but instead defines the weighted mean, consistent with the extrapolations in *McCarthy et al.* [2004]. The estimated

Table 2. Tropical (20°S–20°N) Zonal Mean Lower Stratospheric (180–50 mb) Water Vapour Minima (ppmv)

Run	January	July	Annual
ORIG	3.18	3.75	4.07
ENT10	3.47	3.65	4.03
ICE	3.32	3.65	4.03
OZONE	2.84	3.04	3.39
STRAT	3.29	3.52	3.71
NEW	2.68	3.00	3.21

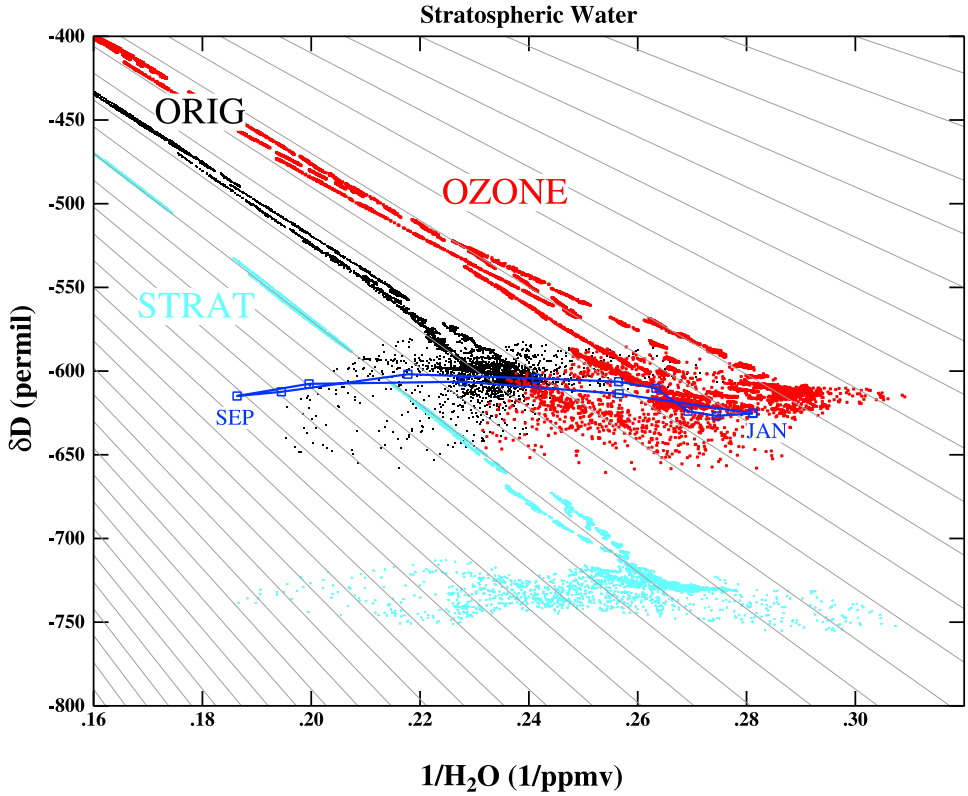

Figure 8. Deuterium (HDO) (‰) ratios as a function of the inverse of the water vapour mixing ratio for a number of single years in selected experiments (ORIG, STRAT and OZONE). Points are from all latitudes and longitudes above 110 mb (117 mb in the STRAT case). The background grid shows lines of constant Ω that thus represent pure mixing lines with methane-derived stratospheric water. The dark blue set of points is the tropical mean seasonal cycle at 95 mb in the ORIG experiment. Our estimate of the weighted mean effective entry values for each experiment lie on the intersection of these lines and the upper stratospheric mean Ω (Table 3).

error in the water vapour value is around 0.1 ppmv, which is a function of the inter-annual variability or whether we use HDO or $H_2^{18}O$. Variations in the isotope entry values are around ±5‰ for δD and ±2‰ for $\delta^{18}O$ (except for STRAT where variations are about twice as large).

[48] The results in Table 3 show that the effective entry values of water are slightly higher than the annual mean minimum (Table 2), and can be compared with the 4.0 ± 0.1 ppmv value derived by *McCarthy et al.* [2004]. The isotopic values in the 20-layer runs range from −620 to −606‰ and −102 to −91‰ for δD and $\delta^{18}O$ respectively. These are uniformly heavy compared to the values inferred from observations. However, the STRAT model has the most depleted values, especially in δD, even though it does not have the driest air. This underlines the importance of processes within the TTL, where the air is drying but also becomes less depleted, presumably due to the presence of isotopically heavy ice.

6. Discussion

[49] We have shown that GCM simulations that only contain the physics of Rayleigh distillation and mixing (through various processes) simulate stratospheric water isotope ratios significantly higher than for pure Rayleigh distillation. We have used the derived quantity Ω (conserved

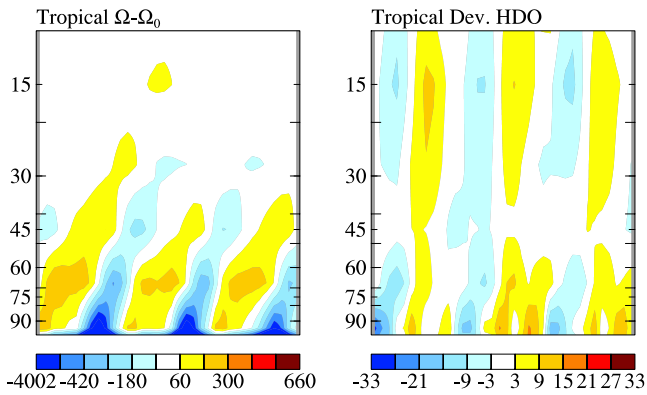

Figure 9. (a) Time-height plot showing the tropical mean (28°S–28°N) values of Ω − Ω_0 in the NEW simulation showing water sources progressing up through the stratosphere. Blue values (more negative Ω) denote wetter source conditions, associated with NH summer conditions. (b) The tropical mean δD anomalies (from the mean at that level) over a period of 3 years. Lower stratospheric conditions mainly reflect the source characteristics, but further up are more affected by the changes in the age of air (which imply varying contributions of methane-derived water).

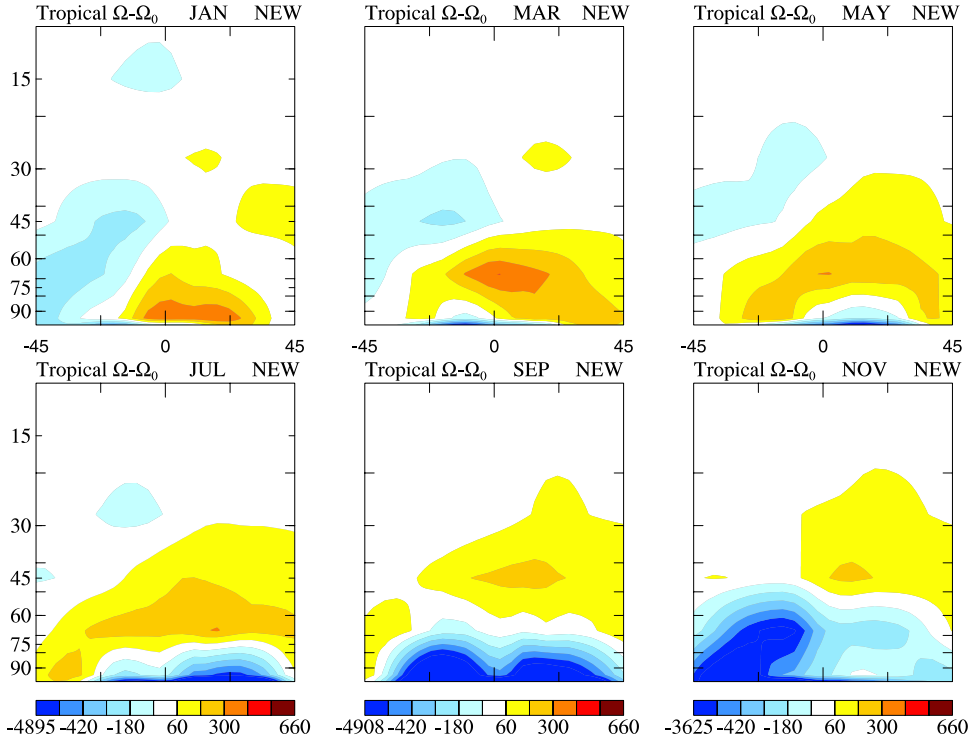

Figure 10. Zonal mean values of $\Omega - \Omega_0$ over a year (every two months) (as in Figure 9). Gradual ascent is clearly seen with almost complete mixing by the time the parcels ascend to 20 mb.

in these simulations) to examine the pathways and mixing of stratospheric water vapour in an analogous way to the use of total H_2 in the real world. The modeled source values for HDO are close to those inferred from the best observational estimates, but not as low in the 20-layer simulations (−600−−620‰), and too depleted in the 23-layer STRAT model (≈−750‰). The source values for $\delta^{18}O$ appear to be uniformly too heavy for the corresponding δD values compared to observations. However the observed $\delta^{18}O$ precision is significantly worse than for δD, and so it is not yet clear whether this is significant.

[50] The largest differences are between the ORIG and STRAT runs which differ in vertical resolution, model top and gravity wave drag scheme. Further experiments (not shown) that are intermediate to ORIG and STRAT demonstrate that the key difference is the slightly higher resolution in the upper troposphere in STRAT. The addition of the GWD scheme and the increase in model top greatly affect the stratospheric turnover time and latitudinal gradients of water vapour but do not substantially impact the processes near the tropopause. While the dependence on upper troposphere vertical resolution is unsatisfying, it does highlight an important, yet poorly constrained, feature of the model. It also confirms that the upper tropospheric and TTL processes are key to understanding the stratospheric entry values, consistent with the results from the sensitivity experiments ENT10 and ICE. In the future, we will perform experiments with significantly higher resolution in this region to further examine this sensitivity.

[51] Previous authors have assumed the troposphere acts as a simple Rayleigh distillation column with no mixing, and argued for the necessity of significant contributions to the stratospheric water budget from lofted ice or overshooting deep convection [*Keith*, 2000; *Sherwood and Dessler*, 2001]. At minimum, the results presented here imply that the no-mixing model for the isotopes is probably not a good basic assumption. Thus while we do not (at present) include the impacts of ice lofting or overshooting convection as possible mechanisms for increasing

Table 3. Values of $\Omega = Q(\delta - \delta_M)$ for Tropical Stratospheric Water Vapour and Ranges of Tropospheric Entry Values

Run	$-\Omega_{HDO}$ Mean 20 mb	$-\Omega_{HDO}$ Range 95 mb	Q_{trop}, ppmv	δD_{trop}, ‰	$\delta^{18}O_{trop}$, ‰
ORIG	2280	1980–2920	4.2	−607	−97
ENT10	2310	2100–2950	4.1	−620	−102
ICE	2240	2000–2900	4.15	−606	−97
OZONE	2020	1750–2700	3.65	−620	−101
SUPSAT	2200	1970–2850	4.2	−597	−91
CAPPA	2290	2020–2970	4.2	−607	−96
STRAT	2500	1970–2850	3.7	−747	−128
NEW	1900	1650–2750	3.5	−610	−95

stratospheric water vapour, we can say that estimates of their importance may have been exaggerated.

[52] However, it is conceivable (particularly for the 20-layer runs) that the GCM over-predicts mixing (and thus the modifications to the pure Rayleigh model) because of numerical effects. Essentially, the model smooths horizontal variations in water vapour ratios over a grid box at every (30 minute) time step. These variations in the real world can arise through small-scale convective plumes, or the shearing of large scale gradients by the horizontal wind field. Observations indicate that such sub-grid scale water vapour anomalies can persist for weeks (and possibly months) [*Pierrehumbert and Yang*, 1993], although whether this is important over longer time scales is as yet unclear. Other mixing processes due, for instance, to large scale advection, are better modeled thanks to the high order tracer advection scheme used which minimises numerical diffusion. In addition, the good simulation of horizontal tropospheric isotopic gradients (Figure 1) provides some confidence that the model is not in general over-diffusive, though this may not necessarily apply to the less well-resolved vertical advection. The difference between STRAT and ORIG in this respect is of some concern, and will be addressed in simulations with significantly higher resolution in future.

[53] The uncertainty in the diffusion coefficients and parameterisation of the kinetic fractionation during evaporation highlighted by *Cappa et al.* [2003] also requires further study. Building the diffusion constants directly into the model's surface flux code (by way of the Schmidt number dependence on the humidity roughness length [*Brutsaert*, 1982]) may be an improvement on the current parameterisations (based on *Merlivat and Jouzel* [1979]). Improved modeling of skin and bulk sea temperature differences appears to be of secondary importance.

[54] The simulation of upper tropospheric isotope values is, however, very difficult to validate since they are essentially decoupled from the well-observed isotopic ratios in precipitation. Some surface effects, related to upper tropospheric changes, are seen at high southern latitudes, particularly in the deuterium excess. This has potential implications for the tuning of the super-saturation parameter and understanding of variations in the deuterium excess through time.

[55] In order for the stratospheric water isotopes to be useful for constraining STE, substantially more information is likely to be required from the upper troposphere (for instance from more extensive experiments such as CRYSTAL-FACE [*Webster and Heymsfield*, 2003], or through improved remote sensing). This may hopefully enable us to use stable isotopes to constrain moist convective parameterisations themselves, one of the prime uncertainties in climate simulations. Improving the modeling of transport and settling of condensate in the model by both the large scale advection and within convective plumes is clearly a high priority, and together with better observations, may go some way to perhaps fulfilling the potential of using water isotopes to study the climate system.

[56] **Acknowledgments.** We would like to express our thanks to Jean Jouzel who has been unstinting in support of isotope modeling at GISS. Support for G.A.S. and Y.H. was provided from NSF grant OCE-99-05038 and a GSFC DDF grant. Support for G.A.S. from EGIDE and CEA France during numerous visits to Saclay is also gratefully acknowledged. Conversations with Steve Sherwood, Andy Gettelman, Liz Moyer, Ron Miller, Tony Del Genio, and an anonymous reviewer were extremely helpful in clarifying some aspects of stratospheric and cloud processes. Christopher Cappa was particularly generous in discussions related to isotopic diffusion coefficients.

References

Brutsaert, W. H. (1982), *Evaporation Into the Atmosphere*, D. Reidel, Norwell, Mass.

Cappa, C. D., M. Hendricks, D. J. DePaolo, and R. C. Cohen (2003), Isotopic fractionation of water during evaporation, *J. Geophys. Res.*, *108*(D16), 4525, doi:10.1029/2003JD003597.

Del Genio, A. D., M. S. Yao, W. Kovari, and K. K. Lo (1996), A prognostic cloud water parameterization for general circulation models, *J. Clim.*, *9*, 270–304.

Del Genio, A. D., W. Kovari, M.-S. Yao, and J. Jonas (2005), Cumulus microphysics and climate sensitivity, *J. Clim.*, in press.

Dessler, A. E. (1998), A reexamination of the "stratospheric fountain" hypothesis, *Geophys. Res. Lett.*, *25*, 4165–4168.

Ehhalt, D. H. (1974), Vertical profiles of HTO, HDO and H_2O in the troposphere, *Tech. Rep. NCAR-TN/STR-100*, Natl. Cent. for Atmos. Res., Boulder, Colo. (Corrected data available at http://www.fz-juelich.de/icg/icg-ii/hdo_vertical_profiles)

Ehhalt, D. H., and L. E. Heidt (1973), Vertical profiles of CH_4 in the troposphere and stratosphere, *J. Geophys. Res.*, *78*, 5225–5271.

Evans, S. J., R. Toumi, J. E. Harries, M. P. Chipperfield, and J. M. Russell III (1998), Trends in stratospheric humidity and the sensitivity of ozone to these trends, *J. Geophys. Res.*, *103*, 8715–8725.

Fleming, E. L., C. H. Jackson, R. S. Stolarski, and D. B. Considine (1999), Simulation of stratospheric tracers using an improved empirically based two-dimensional model transport, *J. Geophys. Res.*, *104*, 23,911–23,934.

Forster, P., and K. P. Shine (1999), Stratospheric water vapor changes as a possible contributor to observed stratospheric cooling, *Geophys. Res. Lett.*, *26*, 3309–3312.

Gat, J. R. (1996), Oxygen and hydrogen isotopes in the hydrologic cycle, *Annu. Rev. Earth Planet. Sci.*, *24*, 225–262.

Gettelman, A., and C. R. Webster (2005), Simulations of water isotope abundances in the upper troposphere and lower stratosphere and implications for stratosphere troposphere exchange, *J. Geophys. Res.*, *110*, D17301, doi:10.1029/2004JD004812.

Hansen, J. E., et al. (2002), Climate forcings in Goddard Institute for Space Studies SI2000 simulations, *J. Geophys. Res.*, *107*(D18), 4347, doi:10.1029/2001JD001143.

Hobbs, P. V., and A. L. Rangno (1985), Ice particle concentrations in clouds, *J. Atmos. Sci.*, *42*, 2523–2549.

Hoffmann, G., M. Werner, and M. Heimann (1998), The water isotope module of the ECHAM Atmospheric General Circulation Model - A study on timescales from days to several years, *J. Geophys. Res.*, *103*, 16,871–16,896.

Holton, J. R., and A. Gettelman (2001), Horizontal transport and the dehydration of the stratosphere, *Geophys. Res. Lett.*, *28*, 2799–2802.

Holton, J. R., P. H. Haynes, M. E. McIntyre, A. R. Douglass, R. B. Rood, and L. Pfister (1995), Stratosphere-troposphere exchange, *Rev. Geophys*, *33*, 403–439.

International Atomic Energy Agency (IAEA) (2001), GNIP maps and animations, Vienna. (Available at http://isohis.iaea.org)

Johnson, D. G., K. W. Jucks, W. A. Traub, and K. V. Chance (2001a), Isotopic composition of stratospheric water vapor: Measurements and photochemistry, *J. Geophys. Res.*, *106*, 12,211–12,218.

Johnson, D. G., K. W. Jucks, W. A. Traub, and K. V. Chance (2001b), Isotopic composition of stratospheric water vapor: Implications for transport, *J. Geophys. Res.*, *106*, 12,219–12,226.

Joussaume, S., and J. Jouzel (1993), Paleoclimatic tracers: An investigation using an atmospheric general circulation model under ice age conditions: 2. Water isotopes, *J. Geophys. Res.*, *98*, 2807–2830.

Joussaume, S., R. Sadourny, and J. Jouzel (1984), A general circulation model of water isotope cycles in the atmosphere, *Nature*, *311*, 24–29.

Jouzel, J. (1986), Isotopes in cloud physics: Multiphase and multistage condensation processes, in *Handbook of Environmental Isotope Geochemistry*, vol. 2, edited by P. Fritz and J. C. Fontes, pp. 61–112, Elsevier, New York.

Jouzel, J., G. L. Russell, R. J. Suozzo, R. D. Koster, J. W. C. White, and W. S. Broecker (1987), Simulations of HDO and $H_2{}^{18}O$ atmospheric cycles using the NASA GISS general circulation model: The seasonal cycle for present-day conditions, *J. Geophys. Res.*, *92*, 14,739–14,760.

Jouzel, J., R. D. Koster, R. J. Suozzo, G. L. Russell, J. W. C. White, and W. S. Broecker (1991), Simulations of HDO and $H_2{}^{18}O$ atmospheric cycles using the NASA GISS general circulation model: Sensitivity experiments for present-day conditions, *J. Geophys. Res.*, *96*, 7495–7507.

Jouzel, J., R. D. Koster, R. J. Suozzo, and G. L. Russell (1994), Stable water isotope behavior during the Last Glacial Maximum: A general circulation model analysis, *J. Geophys. Res.*, *99*, 25,791–25,801.

Keith, D. W. (2000), Stratospheric-tropospheric exchange: Inferences from the isotopic composition of water vapor, *Geophys. Res. Lett.*, *105*, 15,167–15,173.

Kuang, Z., G. C. Toon, P. O. Wennberg, and Y. L. Yung (2003), Measured HDO/H_2O ratios across the tropical tropopause, *Geophys. Res. Lett.*, *30*(7), 1372, doi:10.1029/2003GL017023.

Mathieu, R., D. Pollard, J. E. Cole, J. W. C. White, R. S. Webb, and S. L. Thompson (2002), Simulation of stable water isotope variations by the GENESIS GCM for modern conditions, *J. Geophys. Res.*, *107*(D4), 4037, doi:10.1029/2001JD900255.

McCarthy, M. C., K. A. Boering, T. Rahn, J. Eiler, A. L. Rice, S. C. Tyler, S. Schauffler, E. Atlas, and D. G. Johnson (2004), The hydrogen isotopic composition of water vapor entering the stratosphere inferred from high-precision measurements of δD-CH_4 and δD-H_2, *J. Geophys. Res.*, *109*, D07304, doi:10.1029/2003JD004003.

McPhee, M. G. (1992), Turbulent heat flux in the upper ocean under sea ice, *J. Geophys. Res.*, *97*, 5365–5379.

Merlivat, L., and J. Jouzel (1979), Global climatic interpretation of the deuterium-oxygen 18 relationship for precipitation, *J. Geophys. Res.*, *84*, 5029–5033.

Mote, P. W., et al. (1996), An atmospheric tape recorder: The imprint of tropical tropopause temperatures on stratospheric water vapor, *J. Geophys. Res.*, *101*, 3989–4006.

Moyer, E. J., F. W. Irion, Y. L. Yung, and M. R. Gunson (1996), ATMOS stratospheric deuterated water and implications for troposphere-stratosphere transport, *Geophys. Res. Lett.*, *23*, 2385–2388.

Noone, D., and I. Simmonds (2002), Associations between $\delta^{18}O$ of water and climate parameters in a simulation of atmospheric circulation 1979–1995, *J. Clim.*, *15*, 3150–3169.

Petit, J. R., J. W. C. White, N. W. Young, J. Jouzel, and Y. S. Korotkevich (1991), Deuterium excess in recent Antarctic snow, *J. Geophys. Res.*, *96*, 5113–5122.

Petit, J. R., et al. (1999), Climate and atmospheric history of the past 420,000 years from the Vostok ice core, *Nature*, *399*, 429–436.

Pierrehumbert, R. T., and H. Yang (1993), Global chaotic mixing on isentropic surfaces, *J. Atmos. Sci.*, *50*, 2462–2480.

Pollack, W., L. E. Heidt, R. Lueb, and D. H. Ehhalt (1980), Measurement of stratospheric water vapor by cryogenic collection, *J. Geophys. Res.*, *85*, 5555–5568.

Prather, M. J. (1986), Numerical advection by conservation of second order moments, *J. Geophys. Res.*, *91*, 6671–6680.

Randel, D. L., F. Wu, S. Oltmans, K. Rosenlof, and G. E. T. Nedoluha (2004), Interannual changes of stratospheric water vapor and correlations with tropical tropopause temperatures, *J. Atmos. Sci.*, *61*, 2133–2148.

Ridal, M., and D. E. Siskind (2002), A two-dimensional simulation of the isotopic composition of water vapor and methane in the upper atmosphere, *J. Geophys. Res.*, *107*(D24), 4807, doi:10.1029/2002JD002215.

Rind, D., and J. Lerner (1996), Use of on-line tracers as a diagnostic tool in general circulation model development: 1. Horizontal and vertical transport in the troposphere, *J. Geophys. Res.*, *101*, 12,667–12,683.

Rind, D., R. Suozzo, and N. K. Balachandran (1988), The GISS global climate/middle atmosphere model. Part II: Model variability due to interactions between planetary waves, the mean circulation, and gravity wave drag, *J. Atmos. Sci.*, *45*, 371–386.

Rosenlof, K. H., et al. (2001), Stratospheric water vapor increases over the past half-century, *Geophys. Res. Lett.*, *28*, 1195–1198.

Rozanski, K., and C. Sonntag (1982), Vertical distribution of deuterium in atmospheric water vapour, *Tellus*, *34*, 134–141.

Rozanski, K., L. Araguás-Araguás, and R. Gonfiantini (1993), Isotopic patterns in modern global precipitation, in *Climate Change in Continental Isotopic Records*, *Geophys. Monogr. Ser.*, vol. 78, edited by P. K. S. et al., AGU, Washington, D. C.

Russell, G. L., and J. A. Lerner (1981), A new finite-differencing scheme for the tracer transport equation, *J. Appl. Meteorol.*, *20*, 1483–1498.

Schmidt, G. A., et al. (2005), Present day atmospheric simulations using GISS ModelE: Comparison to in-situ, satellite and reanalysis data, *J. Clim.*, in press. (Available at http://www.giss.nasa.gov/tools/modelE)

Sherwood, S. C., and A. E. Dessler (2001), A model for transport across the tropical tropopause, *J. Atmos. Sci.*, *58*, 765–779.

Shindell, D. T. (2001), Climate and ozone response to increased stratospheric water vapor, *Geophys. Res. Lett.*, *28*, 1551–1554.

Smith, R. B. (1992), Deuterium in North Atlantic storm tops, *J. Atmos. Sci.*, *49*, 2041–2057.

Webster, C. R., and A. J. Heymsfield (2003), Water isotope ratios D/H, $^{18}O/^{16}O$, $^{17}O/^{16}O$ in and out of clouds map dehydration pathways, *Science*, *302*, 1742–1745. (Corrected data available at espoarchive.nasa.gov/archive/arcs/crystalf)

Werner, M., M. Heimann, and G. Hoffmann (1998), Stable water isotopes in Greenland ice cores: ECHAM4 model simulations versus field measurements, in *International Symposium on Isotope Techniques in the Study of Past and Current Environmental Changes in the Hydrosphere and the Atmosphere*, pp. 603–612, Int. At. Energy Agency, Vienna.

Wick, G. A., W. J. Emery, L. H. Kantha, and P. Schlussel (1996), The behavior of the bulk-skin sea surface temperature difference under varying wind speed and heat flux, *J. Phys. Oceanogr.*, *26*, 1969–1988.

Yao, M. S., and A. D. Del Genio (1989), Effects of cumulus entrainment and multiple cloud types on a January global climate model simulation, *J. Clim.*, *2*, 850–863.

Zahn, A. (2001), Constraints on 2-way transport across the Arctic tropopause based on O_3, stratospheric tracer (SF_6) ages, and water vapor isotope (D, T) tracers, *J. Atmos. Chem.*, *39*, 303–325.

Zahn, A., V. Barth, K. Pfielsticker, and U. Platt (1998), Deuterium, tritium and oxygen-18 as tracers for water vapour transport in the lower stratosphere and tropopause region, *J. Atmos. Chem.*, *30*, 25–47.

G. Hoffmann, LSCE/CEA, Orme des Merisiers, 91191 Gif sur Yvette, France. (hoffmann@lsce.saclay.cea.fr)

Y. Hu, Department of Atmospheric Sciences, Peking University, 100871 Beijing, China. (yongyunhu@pku.edu.cn)

G. A. Schmidt and D. T. Shindell, NASA Goddard Institute for Space Studies and Center for Climate Systems Research, Columbia University, 2880 Broadway, New York, NY 10025, USA. (gschmidt@giss.nasa.gov; dshindell@giss.nasa.gov)